Meta-omic insights into active bacteria mediating N_2O mitigation and dissimilatory nitrate reduction to ammonium in an ammonia recovery bioreactor

Hop V. Phan, [1] Shohei Yasuda,[2, 3] Kohei Oba,[1] Hiroki Tsukamoto,[1] Tomoyuki Hori,[4] Megumi Kuroiwa,[1] Akihiko Terada[1,2]

[1.] Department of Applied Physics and Chemical Engineering, Tokyo University of Agriculture and Technology, 2-24-16 Naka-Cho, Koganei, Tokyo, 184-8588, Japan

[2.] Global Innovation Research Institute, Tokyo University of Agriculture and Technology, 3-8-1 Harumi-Cho, Fuchu, Tokyo, 185-8538, Japan

[3.] Department of Civil Engineering, University of Galway, University Road, Galway, H91 TK33, Ireland

[4.] Environmental Management Research Institute, National Institute of Advanced Industrial Science and Technology, 16-1 Onogawa, Tsukuba, Ibaraki, 305-8569, Japan

*Corresponding author: akte@cc.tuat.ac.jp

Competing Interests statement: There is no competing interest.

Abstract

Shifting from ammonia removal to recovery is the current strategy in wastewater treatment management. We recently developed a microaerophilic activated sludge (MAS) system for retaining ammonia while removing organic carbon with minimal N_2O emissions. A comprehensive understanding of nitrogen metabolisms in the MAS system is essential to optimize system performance. Here, we employed metagenomics and metatranscriptomics analyses to characterize the microbial community structure and activity during the transition from a microaerophilic to an aerobic condition. A hybrid approach of high-quality Illumina short reads and Nanopore long reads recovered medium- to high-quality 98 non-redundant metagenome-assembled genomes (MAGs) from the MAS communities. The suppressed bacterial ammonia monooxygenase (*amoA*) expression was upregulated after shifting from a microaerophilic to an aerobic condition. The 73 MAGs (>74% of the total) from 11 bacterial phyla harbored genes encoding proteins involved in nitrate respiration; 39 MAGs (~53%) carried N_2O reductase (*nosZ*) genes with the predominance of clade II *nosZ* (31 MAGs), and 24 MAGs (~33%) possessed nitrite reductase (ammonia forming) genes (*nrfA*). Clade II *nosZ* and *nrfA* genes exhibited the highest and second-highest expressions among nitrogen metabolism genes, indicating robust N_2O consumption and ammonification. Non-denitrifying clade II *nosZ* bacteria, *Cloacibacterium* spp., in the most abundant and active phylum Bacteroioda, were likely major N_2O sinks. Elevated dissolved oxygen (DO) concentration inhibited clade II *nosZ* expression but not *nrfA* expression, potentially switching phenotypes from N_2O reduction to ammonification. Collectively, the multi-omics analysis illuminated vital bacteria responsible for N_2O reduction and ammonification in microaerophilic and aerobic conditions, facilitating high-performance ammonia recovery.

Keywords: Ammonia retention; Dissimilatory nitrate reduction to ammonia; Metagenomics; Metatranscriptomics; Nitrous oxide

INTRODUCTION

In conventional wastewater treatment plants, nitrogen in wastewater is removed by converting reactive nitrogen into dinitrogen gas via nitrification-denitrification. While this process alleviates the environmental burden associated with nitrogen constituents, the requirements of energy-intensive aeration, external organic carbon, and waste sludge disposal make the process incompatible with sustainable development goals [1, 2]. A transition from nitrogen removal to recovery was initiated in wastewater treatment plants toward sustainable nitrogen management. Ammonia recovery from high-strength nitrogenous organic wastewater ensures energy stored in ammonia, overcoming the high energy demand in conventional nitrogen removal and preventing the emission of nitrous oxide (N_2O), which is a potent greenhouse gas with a global warming potential 273 times higher than that of CO_2 and accounts for nearly 80% of the total CO_2 footprint of a wastewater treatment plant (WWTP) [3].

We recently developed a microaerophilic activated sludge (MAS) system to retain ammonia in nitrogenous wastewater while removing organic carbon [4, 5]. Setting low dissolved oxygen (DO) concentrations (< 0.1 mg/L) and short solids retention times (SRT) (< 5 d) in a MAS system out-selects nitrifying bacteria for suppressing ammonia oxidation, which saves energy and prevents N_2O emissions. In contrast, the fluctuation of influent nitrogen loadings increases oxygen concentrations, initiating nitrification and producing N_2O in the system [5]. Understanding the microbial community and functions regarding carbon and nitrogen metabolisms in the MAS system is essential to optimize the system operation for removing organic carbon, enriching ammonia, and mitigating N_2O emissions.

Mitigating N_2O emission entails a better understanding of N_2O-reducing bacteria. N_2O-reducing bacteria reduce N_2O to N_2 anaerobically by a copper-dependent N_2O reductase (NosZ) [6]. This enzyme is phylogenetically classified into two clades, which differ in *nos* gene clusters, translocation (clade I) or secretory (clade II) pathways [7, 8]. Clade I *nosZ* is typically present in canonical denitrifiers possessing an entire set of denitrifying genes. Over half of the bacteria containing clade II *nosZ* are non-denitrifiers, missing genes encoding nitrate and nitrite reductases [9]. Studies reported higher abundances of clade II *nosZ* bacteria in soils and WWTPs than clade I *nosZ* bacteria [7, 10], likely because of their higher competitiveness and energy efficiency under N_2O-limited conditions. These physiological traits, however, have been controversial, claiming higher growth yields and N_2O affinities of clade II *nosZ* bacteria [11-13] and *vice versa* [14, 15]. Thus, understanding clade I and II *nosZ* ecophysiologies is indispensable

for N_2O mitigation. Exploring active N_2O-reducing bacteria under microaerophilic conditions in the MAS system is crucial for the sustainable mitigation of sporadically occurring N_2O emission [5] as the MAS system employs a microaerophilic condition. Recently, multiple phenotypes of N_2O reduction in the presence of oxygen, *i.e.*, intolerant, sensitive, and tolerant trends, were reported [12, 16-19]. Their complex phenotypes, nevertheless, are still under debate.

Bacteria exerting dissimilatory nitrate reduction to ammonia (DNRA) are likely key guilds in the MAS system for improving ammonia recovery. These bacteria possess pentaheme *c*-type (c552) cytochrome nitrite reductase (encoded by *nrfA* genes), NADH-dependent nitrite reductases (encoded by *nirB* genes), or octaheme tetrathionate reductase (encoded by *octR* genes) [20, 21]. Despite the ubiquitous presence of DNRA bacteria, studies of DNRA in WWTPs have been limited. Wang et al. [22] reported a lower abundance and activity of DNRA than denitrifying bacteria in WWTPs. Applying their functions in ammonia recovery [23, 24] requires more research.

Bacteria performing both N_2O reduction and DNRA could be harnessed in the MAS system. Nearly one-third of non-denitrifiers with clade II *nosZ* also possess *nrfA*, suggesting the omnipresence of these specialized bacteria in the environment [8]. Pure culture works revealed the growth conditions and regulatory mechanisms between DNRA and denitrification (canonical denitrifiers) or N_2O respiration (non-denitrifiers) [25-27]. Nevertheless, knowledge about the N_2O-reducing and DNRA specialists, especially in engineered systems, is scarce. A comprehensive understanding of the intricate genotypes and transcripts of these specialists may allow the development of conditions to maximize N_2O reduction and DNRA activities, enhancing the ammonia recovery performance of the MAS systems.

This study used a meta-omics approach by hybrid sequencing to elucidate the ecophysiologies of nitrogen-transforming microorganisms in a MAS system. Characterizing the microbial community structure and activity under microaerophilic and oxygen-elevating conditions is essential to manage the MAS system. We hypothesized that (i) the activity of N_2O reducers is compromised at an elevated DO concentration, activating ammonia-oxidizing microorganisms (AOMs) to emit N_2O; (ii) the microbial guilds responsible for N_2O reduction contribute to the mitigation of N_2O emission under microaerophilic conditions; and (iii) DNRA bacteria possess the metabolic potential of N_2O reduction. To examine these hypotheses, the objectives of this

study were as follows: (1) to reveal which AOMs are responsible for nitrification at an elevated DO concentration; (2) to characterize the bacteria actively reducing nitrogen oxides, particularly N_2O under microaerobic and aerobic conditions; and (3) to unravel the phylogeny of bacteria exerting N_2O-reducing and DNRA in the MAS system.

MATERIALS AND METHODS

Bioreactor operation and sampling

Two parallel MAS systems (R1 and R2) were operated for nearly 300 days. These systems were designed to retain ammonia and remove organic matter from high-strength nitrogenous wastewater by suppressing ammonia oxidation and minimizing N_2O emissions. The operation, performance, 16S rRNA gene-based microbial profiles, and qPCR of functional genes of the systems over time were previously reported [5]. Biomass samples were collected in triplicate from R2 on day 268 under microaerophilic (control) conditions with an aeration rate of 2.0 L/min and DO of < 0.02 mg/L. The aeration rate doubled (4 L/min), concomitantly increasing DO concentration. After 19 h, triplicate biomass samples for metatranscriptomics were collected. Aeration rate, DO concentration, NH_4^+, and NO_3^- concentrations were recorded every minute by a DO electrode (MultiLine® Multi 3510 IDS Multi-Parameter Portable Meter, WTW, Germany) and NH_4^+/NO_3^- sensors (VARiON plus 700 IQ, WTW). Off-gas N_2O concentration was measured by GC-MS (GCMS-QP2010 SE, Shimadzu, Kyoto, Japan). These data are presented in **Supplementary Fig. S1**.

DNA/RNA extraction and Illumina sequencing

Fresh biomass samples were subjected to DNA extraction using a Fast DNA spin kit for soil and a FastPrep-24 instrument (MP-Biomedicals, Santa Ana, CA, USA) following the manufacturer's protocol. DNA quality was checked by 1% agarose gel electrophoresis and a spectrophotometer (NanoDrop 2000, ThermoFisher Scientific, MA, USA). DNA concentration was determined with the Qubit dsDNA HS Assay Kit (Thermo Fisher Scientific, Waltham, MA, USA) and diluted to 50 ng/μL. Sequencing libraries were prepared with the MGIEasy FS PCR Free DNA library prep set (MGI Tech, Shenzhen, China) following the manufacturer's protocol. The 150-bp paired-end sequencing was performed using DNBSEQ-G400RS (MGI Tech).

Prior to RNA extraction, biomass samples were immediately immersed into RNA*later*® RNA Stabilization Reagent (Thermo Fisher Scientific). Briefly, 50 mL activated sludge was sampled and centrifuged at 3000 rpm for 30 s. The supernatant was pipetted out to leave 1 mL, and the residue was mixed with 10 mL of RNA*later* reagent in 15 mL tubes. The mixture was kept at 4°C for 24 h and then stored at -20°C. Following the manufacturer's protocol, total RNA was extracted using a FastRNA Pro Blue kit (MP Biomedicals, CA, USA). After depleting rRNA with a NEBNext rRNA Depletion Kit (Bacteria) (New England Biolabs, MA, USA) and confirming DNA concentrations were below the detection limit, fragmented 250-bp RNA was used for preparing complementary DNA sequencing libraries with the MGIEasy RNA Directional Library Prep Set (MGI Tech) following the manufacturer's protocol. The sequencing was performed with DNBSEQ-G400RS (MGI Tech). DNA and RNA short-read sequencing was conducted by Genome-Lead Co., Ltd (Tokyo, Japan).

High molecular weight (HMW) DNA extraction and nanopore sequencing

For long-read nanopore sequencing, DNA was extracted from R2 biomass samples in duplicate using a phenol-chloroform method [28]. RNA was removed by RNase, and genomic DNA was precipitated and washed with ice-cold ethanol. Extracted DNA was resuspended in TE buffer and stored at 4°C. The integrity and purity of extracted DNA were checked by 1% agarose gel electrophoresis and a Nanodrop spectrophotometer. The extracted DNA concentration and purity were quantified by a Qubit Assay.

HMW DNA (1 µg) was subjected to library preparation using the ligation sequencing kit SQK-LSK109 (Oxford Nanopore Technologies, Oxford, United Kingdom). Following the manufacturer's protocol, Nanopore sequencing was performed using a MinION Mk1B instrument (R.9 flow cell, FLO-MIN106; Oxford Nanopore Technologies). Base calling was conducted after sequencing using Guppy software version 5.0.11 (Oxford Nanopore Technologies).

Metagenomic assembly

Quality control of paired-end short reads (SR) was performed by Fastp (v 0.20.1) [29] with specific parameters (-q 30 -n 20 -t 1 -T 1 -l 30). After quality control, more than 35 million pairs and 31 million pairs of reads were obtained for R1 and R2, respectively. The quality-filtered SR

from R1 and R2 samples were assembled individually using Megahit (v1.2.9) with parameters (--k-min 21 –k-max 141 –k-step 12).

Nanopore sequencing produced 970718 sequences, with the longest sequence of 261486 bp and a mean read length of 5981 bp; 100% reads were above Q7, and more than 85% reads were above Q10. The raw reads were directly subjected to assembly using Flye (v2.9-b1768) with the "-meta" setting and the "-nano-hq" mode. The quality-filtered SR were mapped to the assembled contigs of long reads (LR) using Burrows-Wheeler Aligner (BWA)-MEM (v0.7.17-r1188) [30] with default parameters. The resulting sequence alignment and map (SAM) files were converted to binary alignment and map (BAM) files and subsequently sorted using SAMtools (v1.14) [31]. The sorted BAM files were used for polishing the assembly of LR using Pilon v1.24 [32] with the option "—fix bases."

Recovery of metagenome-assembled genomes (MAGs)

MAGs from R1 and R2 were recovered as previously described [33] with some modifications. Briefly, the polished contigs of LR assembly were merged with the assembled contigs of paired-end SR (individually for R1 and R2) using the function Merge_wrapper.py in Quickmerge (v0.3) [34] with parameters (-ml 7500 -c 3 -hco 8). The merged results were then processed individually for each sample. Automatic binning was performed using MetaWRAP (v1.3.2) [35] binning module with three genome binners: Concoct [36], Maxbin2 [37], and Metabat2 [38]. Additional binning was done with Vamb (v3.0.2) [39]. The bins from all binning tools were consolidated using the Bin_refinement module (parameters: -c 50 -x 10) of MetaWRAP (v1.3.2). The subsequent steps included extraction of SR and LR for the individual bin, reassembly of LR for each bin and reassembly of each bin, and bin polishing, as described elsewhere [33]. The final bins, MAGs, were selected on the basis of quality (completeness – 5 × contamination > 50) [40] determined by CheckM (v1.1.3).

MAGs from both R1 and R2 were combined and dereplicated using dRep (v3.2.2) [41] (-p 32 -l 2000 -pa 0.90 -sa 0.99 -comp 50 -con 10 -nc 0.1). The processed MAGs were first divided into primary clusters using Mash at a 90% Mash average nucleotide identity (ANI) (specified by -pa 0.90). Each primary cluster was then used to form secondary clusters at the threshold of 99% ANI (-sa 0.99) with at least 25% overlap between genomes. The best MAG was selected within each cluster on the basis of completeness, redundancy, N50 of contigs, and fragmentation. MAG

taxonomic assignment was obtained using the "classify_wf" workflow of GTDB-Tk (v2.4.0) [42] with the Genome Taxonomy Database (GTDB) R220 [43].

Metatranscriptomics processing

The remaining adapter sequences in metatranscriptomic data were trimmed with trim galore (v0.6.6) (https://www.bioinformatics.babraham.ac.uk/projects/trim_galore/). Quality control of paired-end metatranscriptomic reads was then processed using the trimFilterPE function of FastqPuri (v1.0) [44] with specified parameters (--length 150 -q 20 -m 20 -Q ENDS -z yes). The rRNA reads in the quality-trimmed reads were filtered out using SortMeRNA (v4.3.4) [45] with the SILVA database (16S and 23S for bacteria and archaea; 18S and 28S for eukaryotes) and Rfam database (5S and 5.8S).

Annotation and functional analysis

All MAGs were annotated using Prokka [46]. Metabolic profiles of MAGs were also generated with the METABOLIC-C.pl program in METABOLIC software [47]. The functional marker genes encoding key enzymes responsible for N-cycle were searched from both Prokka annotation and HMM search results of METABOLIC. The markers' nucleotide and amino acid sequences were extracted using the "Subseq" function of Seqtk (https://github.com/lh3/seqtk). The results were compared, manually curated, *i.e.,* length, locus position, and presence of other genes in the operons, and confirmed by Blastp amino acid sequences against NCBI nr databases. Genes encoding putative high-affinity terminal oxidases (cytochrome bd ubiquinol oxidases *cydAB* and cbb3-type cytochrome c oxidases *ccoNO*) and low-affinity terminal oxidases (caa3-type cytochrome c oxidases *coxAB*) were obtained from MAGs [48].

The *amoA* genes encoding ammonia monooxygenase were not found in any recovered MAGs. To conduct a more comprehensive search of *amoA* gene, HMM profiles of *amoA*- ammonia-oxidizing archaea (AOA) (archaeal *amoA*), *amoA*- ammonia-oxidizing bacteria (AOB) (bacterial *amoA*), and *amoA*- complete ammonia-oxidizing bacteria (comammox) (*Nitrospira* comammox *amoA*) were downloaded from Fungene [49]. Hmmsearch using these profiles was conducted against all contigs (> 500 bp), and the results were checked by Blastp.

Universal single copy marker (SCM) genes were extracted using the fetchMGs tool (available at https://motu-tool.org/fetchMG.html). A subset of 10 SCMs (COG0012, COG0016, COG0018, COG0172, COG0215, COG0495, COG0525, COG0533, COG0541, COG0552) were selected following previous studies [17, 50]. The median transcript abundance of these 10 SCMs was applied to estimate the transcription activity of the MAG [50, 51].

Calculating relative abundance and mRNA expression

The quality-filtered metagenomic SR and non-rRNA metatranscriptomic reads of each sample were mapped to all dereplicated MAGs using BWA-MEM (v0.7.17-r1188) [30] with the default setting. The unmapped reads were filtered out with SAMtools view (-hbS -F4), and the BAM file was subsequently sorted with SAMtools sort. The coverage of each MAG was calculated using the "genome" mode of coverM (v0.6.1) (https://github.com/wwood/CoverM) with the transcripts per million (TPM) method [52].

To calculate the abundance and mRNA expression of functional marker genes, the reads were mapped against the extracted nucleotide sequences using bowtie2 [53] in "-very-sensitive" mode (to ensure unique mapping). The mapped reads were filtered and sorted as described above. The coverages of marker genes in each sample were obtained by the "contig" mode of coverM (v0.6.1) (https://github.com/wwood/CoverM). The TPM values were normalized to total reads mapped to a sample. The raw-read count was obtained from coverM (v0.6.1) with the "count" method for statistical analysis of the differential mRNA expression using DESeq2 [54].

Phylogenomic analyses of MAGs and phylogenetic analyses of functional genes

To construct the phylogenetic tree of MAGs, the multiple sequence alignment of 120 bacterial marker genes (*gtdbtk.bac120.user_msa.fasta*) identified and generated by the "classify_wf" workflow of GTDB-tk (v2.4.0) was used to infer the maximum likelihood phylogenetic tree using IQ-TREE2 (v2.2.0) (-T AUTO -m LG). A Newick tree output file was visualized with iTOL v6 (https://itol.embl.de/).

For functional marker genes, amino acid sequences were clustered at a 95% similarity threshold using CD-hit. The corresponding references for each marker are presented in **Table S1**. The amino acid sequence clusters and reference sequences were combined and aligned with Muscle

[55] (for the individual key functional genes). The phylogenetic tree was \ with IQ-TREE2 [56] (v2.2.0) (-m MFP -B 1000 -T AUTO). The best model for a phylogenetic tree was selected in accordance with Bayesian information criterion scores and weights (BIC). The tree was visualized with iTOL v6 and used to phylogenetically classify the sequences in this study (**Figs. S2** and **S3**).

Data depositions

The raw 16S rRNA gene amplicon, metagenomic, and metatranscriptomic sequencing data are available in the DNA Data Bank of Japan (DDBJ) nucleotide sequence database under bioproject accession numbers of PRJDB17920, 17921, and 17922, respectively. Assembled and annotated MAGs have been deposited in the DDBJ nucleotide sequence database with the accession numbers SAMD00776737-SAMD00776788. Metatranscriptomic sequencing data have been deposited with the accession numbers SAMD00770009-SAMD00770012.

RESULTS

The dynamics of nitrogen species

The MAS systems were stably operated on day 268, just before the aeration rate was doubled. DO was below the detection limit at an aeration rate of 2 L/min. Gaseous N_2O in the headspace of R2 was 2.6 ppmv, while NO_3^- concentration ranged from undetectable levels to 0.7 mg-N/L (**Fig. S1**). The increase in the aeration rate to 4 L/min for 15 h surged DO concentration to 6.5 mg/L, in conjunction with a linear increase in NO_3^- concentration of 2.8 mg-N/L (**Fig. S1**). The off-gas N_2O concentration increased to 6.5–10.3 ppmv, in line with our previous observation [5]. Decreasing aeration to the original level (2 L/min) plunged DO and NO_3^- concentrations. This stepwise change in aeration activated ammonia oxidation at a high DO concentration and increased N_2O emission when transitioning from anoxic to oxic conditions.

Microbial community structure

Ninety-seven and one non-redundant MAGs belong to Bacteria and Archaea (genus *Methanomassiliicoccus*), respectively. Among these, 53 MAGs were above the criteria, with completeness > 90% and contamination < 5%; the average completeness and contamination were

85.7% and 1.6%, respectively (**Supplementary Text S1** and **Table S2**). In total, 82.4% and 84.3% of high-quality SR from metagenomic data of R1 and R2 samples, respectively, were mapped to the 98 non-redundant MAGs. Additionally, 84.5 ± 0.01% (n=3) and 82.8 ± 0.00% (n=3) non-rRNA metatranscriptomic reads mapped to 98 MAGs for control and high DO samples, respectively, indicating that the recovered MAGs well represented the microbial community in MAS systems.

In an overall comparison, the microbial profiles by the MAGs and by amplicon sequencing of the V4 16S rRNA region displayed a similar composition of the dominant phyla/class (R1_16S *vs.* R1_MG and R2_16S *vs.* R2_MG in **Fig. 1**). A similar trend of the relative abundance at a phylum level (class for Proteobacteria) between R1 and R2 was captured by both methods (R1_16S *vs.* R2_16S and R1_MG *vs.* R2_MG). Higher relative abundances of Gamma- and Alphaproteobacteria were detected in R2 than in R1, while those of Chloroflexota and Bacillota were higher in R1 than in R2 (**Fig. 1**).

In contrast, the 16S rRNA gene data showed higher fractions in Proteobacteria (55.3%–68.7%) and Bacillota (3.8%–9.6%) than MAGs data (24.9%–31.2% for Proteobacteria and 1.1%–1.8% for Bacillota), while the opposite trend was obtained regarding the fractions of Bacteroidota [30.9 %–34.9% (MAG) *vs.* 12.3%–12.7% (16S)] and Chloroflexota [23.8%–28.6% (MAG) *vs.* 10.2%–13.7% (16S)]. Additionally, the metagenomics approach retrieved MAGs affiliated with the families of Ozemobacteraceae, *Candidatus* Hinthialibacteraceae, and JAAZCA01 in three *Candidatus* phyla, Riflebacteria, Hinthialibacterota, and UBA10199, that were not captured by 16S rRNA gene amplicons. The differences are presented in **Text S1**.

The overall response of microbial activity to DO concentration

The metatranscriptomic data showed that Bacteroidota, which are facultative anaerobes [57], was the most active population in the MAS system, accounting for 66.9% of gene expression under the microaerophilic condition; it decreased to 38.3% under high DO conditions (**Fig. 1**). The second and third transcriptionally active groups were Chloroflexota and Gammaproteobacteria, respectively. The transcription activities were two and three times lower in the microaerophilic condition than in the high DO condition for Chloroflexota [15.2% (control) *vs.* 28.7% (high O_2)] and Gammaproteobacteria [6.5% (control) vs. 20.3% (high O_2)], respectively.

The most downregulated population under a high DO condition was Bdellovibrionota (15-fold), followed by Cloacimonadota (5.7-fold). Other bacterial taxa (Riflebacteria, Campylobacterota, and Desulfobacterota) were downregulated by factors of 4.4–4.8. In contrast, increasing DO concentration activated Alphaproteobacteria (26-fold), followed by Actinobacteriota (23-fold), Verrucomicroiota (16-fold), and Gemmatimonadota (9.2-fold).

The predominant and active bacterial members of the MAS systems

Analyzing the relative abundance and RNA expression of the recovered MAGs allowed for predicting the *in situ* contribution of the community members to the system performance. Overall, the predominant and transcriptionally active bacterial species in the MAS system were identical. An unclassified species (UBA8950 R1_bin.54_o, Chloroflexota) was the most prominent MAG (average log_2TPM of 17.5) and was the third and the second most active member under control (log_2TPM of 16.6) and high DO conditions (log_2FC of 0.8), respectively (**Fig. 2**). The following top abundant MAGs are affiliated with Bacteroidota (in decreasing order of average abundance): unclassified species of UBA6192 (R2_bin.12_r, log_2TPM of 16.1), *Cloacibacterium* sp. 002422665 (R1_bin.104_o, log_2TPM of 16.0), and unclassified species of genus *Paludibacter* (R2_bin.117_r, log_2TPM of 15.7). While the activities of these three Bacteroidota members slightly decreased with increasing DO concentrations, *Cloacibacterium* sp. 002422665 was the most active member in the community under both controls (log_2TPM of 18.4) and high DO (log_2TPM of 17.8) conditions. UBA6192 MAG and *Paludibacter* MAG were the top active bacterial species under both conditions (**Fig. 2**). Other abundant bacterial species belong to Gammaproteobacteria (*Rubrivivax, Thermomonas*, and Burkholderiaceae) with an average log_2TPM of 15.0–15.4. *Thermomonas* MAG was the top active member under both conditions, whereas the transcription activities of *Rubrivivax* (R1_bin.6_o) and Burkholderiaceae (R1_bin.59_o) were moderate under microaerophilic conditions (log_2TPM of 12.1 and 11.1, respectively) and significantly upregulated (log_2FC of 2.2 and 3.2, respectively) at a high DO concentration (adj *p-value* < 0.05). The downregulated and upregulated bacterial members at the high DO concentration are provided in **Supplementary Text S2**.

Nitrogen metabolism

Ammonia oxidation

The MAS system aims to retain ammonia by suppressing ammonia oxidation [5]. As expected, an HMM search using hmm profiles of archaeal, bacterial, and comammox AmoA did not return a hit from the 98 recovered MAGs. A comprehensive search against all assembled contigs (> 500 bp) obtained three hits for both bacterial and comammox AmoA profiles (with each contig < 1000 bp), while no hit was returned for the archaeal AmoA profile. The phylogenomic analysis identified them as *Nitrosomonas* AmoA (**Fig. 3**). The presence of *amoA* genes in the metagenomic data was sporadic, with total abundances of 0.16 TPM (R1) and 0.34 TPM (R2). The full expression under the microaerophilic condition was 0.05–1.01 TPM (**Table 1**). Notably, increasing DO concentration dramatically induced the expression of *amoA* genes with a total expression of 22.7–29.1 TPM, which was an average 57.7 times higher than expression in the microaerophilic condition (**Table 1**). This result highlighted the suppressive effect of the microaerophilic condition on AOMs in the MAS systems. A low amount of AOB (*Nitrosomonas*) was present in the system, while AOA and comammox bacteria were absent.

Microbial activity of nitrate respiration in the MAS community

All genes involved in nitrogen oxide respiration were found in the recovered MAGs (**Fig. 4A**). The most abundant gene was *narG* (386-405 TPM), followed by *nrfA* (285-366 TPM), *nirS* (241-242 TPM), and clade II *nosZ* (129-254 TPM). The dominant gene types in reduction of nitrogen oxides were *narG* among nitrate reductase (~5.1 times of *napA*), *nirS* among nitrite reductase (~3.2 times of *nirK*), *cnorB* among nitric oxide (NO) reductase (~1.6 times of *qnorB*), clade II *nosZ* among N_2O reductase (~9.4 times of clade I *nosZ*), and *nrfA* among DNRA (~2.9 times of *octR* and ~19 times of *nirB*). Clade I *nosZ* was the least abundant (18–22 TPM) of all genes for nitrogen oxide reduction.

As for transcripts, clade II *nosZ* was the most highly expressed gene in the control (microaerophilic) condition (2375 ± 282 TPM, n = 3) (**Fig. 4A** and **B**). The second and third most expressed genes were *nrfA* (1130 ± 359 TPM, n = 3) and *nirS* (861 ± 372 TPM, n = 3), respectively, which were approximately 3.5 times as high as the gene abundances (**Fig. 4A** and **B**). Other gene expressions were low, ranging from 0 (*nirB*) to 269 TPM (*qnorB*). The *narG*

transcript was half of its metagenomic abundance under microaerophilic conditions. Clade I *nosZ* and *nirB* genes were scarcely expressed.

Increasing DO concentration significantly repressed the expression of clade II *nosZ* and *cnorB*, which decreased by ~3.8 times (633 ± 91 TPM, n = 3) and ~2.5 times (76 ± 17 TPM) in high DO conditions, respectively. *qnorB* gene expression was kept constant (269 ± 44 TPM and 270 ± 17 TPM under microaerophilic and high DO conditions). In stark contrast, *narG*, *nirS*, and *nifA* gene expressions increased by ~3.0, 1.9, and 1.7 times under high DO conditions, respectively (**Fig. 4A** and **B**). While clade I *nosZ* expression doubled at high DO concentrations, the total expression was negligible (11 ± 4 TPM, n = 3) (**Fig. 4A**).

Microbial sinks of N_2O in MAS systems

Of the 98 recovered MAGs, 73 MAGs (>74%) from 11 bacterial phyla harbor genes involved in nitrate respiration. Of the 73 MAGs, 39 MAGs (~53%) carried *nosZ* genes. The phylogenetic allocation at a genus level is shown in **Fig. S2**. Notably, 31 MAGs harbor clade II *nosZ* and were distributed mainly in Bacteroidota (22 MAGs), followed by Gammaproteobacteria (5 MAGs), Gemmatinomadota (3 MAGs), and Chloroflexota (1 MAG) (**Fig. 5**). Only 8 MAGs carried clade I *nosZ* and consisted exclusively of Alpha- (4 MAGs) and Gammaproteobacteria (4 MAGs). All Alphaproteobacteria MAGs carrying clade I *nosZ* possessed only *nirK* and *cnorB* as denitrifying genes. These MAGs expressed low levels of *nirK* (3.1–5.3 TPM) and generally did not express other genes (**Fig. 5**).

Six MAGs possessed a complete set of denitrification genes, all belonging to the order Burkholderiales (Gammaproteobacteria). These canonical complete denitrifiers harbor *nirS* type (no *nirK* type) and *cnorB* (except for *Thiobacillus* harboring both *cnorB* and *qnorB*). Three complete denitrifying MAGs, *i.e.*, two unclassified *Thiobacillus* species (R1_bin.5_r and R2_bin.72_o) and *Thauera terpenica* (R2_bin.16_o), carried clade I *nosZ*. The other three complete denitrifying MAGs carried clade II *nosZ* (two unclassified UBA2250 species [R1_bin.60_r and R1_bin.67_r] and one unclassified *Thauera* species [R2_bin.50_o]). Notably, the six complete denitrifying MAGs do not have *nrfA* genes, but all contain *octR* genes for DNRA. Regardless of the clade type, all denitrifying genes in these MAGs were expressed at low levels.

Among 31 MAGs harboring clade II *nosZ*, 18 MAGs were non-denitrifying bacteria missing genes encoding nitrate and nitrite reductases (**Fig. 5**). Although the expression level decreased from a microaerophilic to a high DO condition (970 TPM to 250 TPM), the highest expressions levels of clade II *nosZ* were found in two *Cloacibacterium* species (*C. normanense* [R1_bin.29_r] and *Cloacibacterium* sp. 002422665 [R1_bin.104_o]) in both conditions. These two species harbor the *cnorB* gene but no nitrate and nitrite reductase genes (**Fig. S4**). The *cnorB* gene expressions of *Cloacibacterium* sp. 002422665 and *C. normanense* were suppressed at a high DO concentration (< 2 TPM).

The other two non-denitrifying MAGs with the top expressions of clade II *nosZ* were RDXD01 MAG [R2_bin.10_o] and CAISCU01 MAG [R2_bin.44_o] in Bacteroidota (**Fig. 5**). These MAGs possess only *nosZ* gene among denitrifying genes. *nosZ* expression decreased from 92.3 ± 20.9 to 51.8 ± 6.8 TPM (RDXD01 species) and 80.9 ± 9.4 to 20.1 ± 4.0 TPM (CAISCU01 species) upon switching from microaerophilic to high DO conditions.

The uncharacterized UBA6192 species (R2_bin.12_r) in Bacterioidota, possessing clade II *nosZ*, *nirK*, *cnorB*, and DNRA genes (*nrfA* and *octR*), showed the unique gene expression patterns. It displayed marginal expressions of *nirK* and *cnorB* genes. Introducing a high DO condition from the microaerophilic condition suppressed the gene expressions of *nosZ* and *octR*, whereas maintaining the gene expression level of *nrfA* and increasing *nirK* and *cnorB* gene expressions (8.5 ± 0.3 TPM and 25.0 ± 2.5 TPM, respectively).

Microbial source of NO and N_2O in MAS systems

Thermomonas (R1_bin.8_o, Gammaproteobacteria), *Paludibacter* (R2_bin.117_r, Bacteroidota), and *Aliarcobacter* (R2_bin.54_o, Campylobacterota) devoid of *nosZ* genes displayed high expressions of *norB* genes, likely ascribed to N_2O sources in the MAS system. *Thermomonas* showed the highest expressions of both *nirS* (328.4 ± 99.1 TPM) and *qnorB* (134.8 ± 36.1 TPM) under microaerophilic conditions. Both gene expressions decreased by half under high DO conditions (157.3 ± 11.5 TPM for *nirS* and 62.8 ± 5.2 TPM for *qnorB*). *Paludibacter* species possessed only the *qnorB* gene among denitrifying genes, with high expression (121.1 ± 5.3 TPM), and *nrfA* gene, with moderate expression (40.1 ± 4.4 TPM), under microaerophilic

conditions. Both *qnorB* and *nrfA* genes were slightly suppressed (~1.5 times) under high DO conditions.

The potential contribution to the microbial NO sources in the MAS system stemmed from the activities of *Rubrivivax* (R1_bin.6_o, Gammaproteobacteria) and UBA8950 (R1_bin.54_o, Chloroflexota). Both species carried only *narG* and *nirS* among the denitrifying genes. Under the microaerophilic condition, *Rubrivivax* species showed high expressions of *nirS* (309.2 ± 181.2 TPM) and *narG* (58.5 ± 42.5 TPM); these levels were noticeably suppressed by 87% and 68%, respectively, after switching to a high DO condition. In contrast, *nirS* and *narG* gene expressions of UBA8950 species were low under microaerophilic conditions (14.7 ± 13.6 TPM and 20.4 ± 15.1 TPM, respectively) and significantly increased (1344.4 ± 26.1 TPM and 371.7 ± 22.8 TPM, respectively) at high DO concentrations. UBA8950 displayed the same transcription trend of *nrfA* gene, which is addressed in the later section.

DNRA

Among the 73 MAGs carrying nitrate respiration-related genes, 24 MAGs (~33%) possessed the *nrfA* gene; this group mainly comprised Bacteroidota (15 MAGs); others belong to Desulfobacterota (3 MAGs), Chloroflexota (2 MAGs), Gammaproteobacteria (2 MAGs), Gemmatinonadota (1 MAG), and Verrucomicrobiota (1 MAG). The phylogenetic allocation at a genus level is shown in **Fig. S3**. Notably, all 8 MAGs harboring the clade I *nosZ* did not carry the *nrfA*, while 8 MAGs (~26%) of 31 MAGs harboring clade II *nosZ* also carried *nrfA*. Among the claded II *nosZ* MAGs, UBA8950 (R1_bin.54_o, Chloroflexota) actively expressed *nrfA* most. As shown in **Figs. 2** and **5**, this MAG was the most abundant species and harbored *narG* and *nirS* genes. Increasing a DO concentration dramatically upregulated *nrfA* expression, from 445.5 ± 335.5 TPM (microaerophilic condition) to 1849.0 ± 172.3 TPM (high DO concentration), together with the upregulation of *nirS* and *narG* genes (**Fig. 5**). This trend was exclusively observed among the MAGs possessing both *nirS* and *nrfA* for nitrite reduction.

The active DNRA members under microaerophilic conditions were Bacteroidota. *Draconibacterium* (R2_bin.47_o) and PGYU01 (R1_bin.45_o) had high *nrfA* expressions of 222.0 ± 9.9 TPM and 154.2 ± 15.9 TPM, respectively. The other six MAGs of Bacteroidota (one UBA6192, four UTCHB3, and one Paludibacter) expressed *nrfA* in the range of 40.1–62.4 TPM

(**Fig. 5**). Except for UBA6192, *nrfA* expressions from all these MAGs were downregulated under high DO conditions.

Of 15 MAGs with *octR* genes, only 2 (UBA6192 and PGYU01) significantly expressed *octR* gene (178.7 ± 26.7 TPM and 46.3 ± 10.0 TPM, respectively). *octR* expressions were downregulated under a high DO condition. While six Gammaproteobacteria MAGs with an entire set of denitrifying genes harbored *nirB* gene, they did not express *nirB* under both examined conditions.

Growth strategy of microorganisms in MAS systems

The transcripts of genes encoding terminal oxidases, clade II nosZ, and nrfA genes (Fig. 6) were compared to characterize the growth strategies of microorganisms in the MAS system. Briefly, the transcription patterns were diverse. *Cloacibacterium* sp. 002422665 (R1_bin.104_o) showed noticeable expression of high-affinity terminal oxidase *ccoNO* (> 12 times of SCM) and clade II *nosZ* (7 times of SCM) under the microaerophilic condition (**Fig. 6**). The increase in the DO concentration downregulated both *ccoNO* and clade II *nosZ* gene expressions by 2.6 and 3.8 times, respectively. Bacteroidota UBA6192 (R2_bin.12_r) showed higher expressions of clade II *nosZ* and *octR* genes than *ccoNO* under microaerophilic yet not aerobic conditions (**Figs. 5** and **6**). Meanwhile, the expression levels of *nrfA* and *ccoNO* remained relatively constant. Chloroflexota UBA8950 (R1_bin.54_o), possessing *cydAB* devoid of *ccoNO*, upregulated high-affinity terminal oxidase *cydAB*, *nrfA*, and *nirS* genes under a high DO condition, with the SCM expression increased by > 7.0 times (**Figs. 5** and **6**). A higher gene expression of low-affinity oxidases (*coxAB*) and *narG* than SCM was also observed after increasing DO concentration (**Figs. 5** and **6**). The expression patterns of other active members are described in **Supplementary Text S3**.

DISCUSSION

A profound understanding of the microbial community and activity in a MAS system is critical for optimizing the system design and operation for innovative ammonia retention and recovery [5]. This study used hybrid sequencing of high-quality Illumina short-reads and Nanopore long-

reads and recovered MAGs to unravel the phylogeny, functions, and transcriptomic activities of MAS communities. Metagenomics and metatranscriptomics analyses supported our hypotheses, in which: (1) N_2O reduction by non-denitrifying bacteria was compromised under high DO conditions, causing N_2O emission likely by AOB; (2) clade II *nosZ* non-denitrifying bacteria (mainly Bacteroidota) were responsible for N_2O reduction under microaerophilic conditions; and (3) 26% of clade II *nosZ* bacteria (8 out of 31 MAGs) harbor *nrfA*, potentially exerting N_2O consumption and DNRA. We further revealed transcriptionally active bacteria driving nitrogen conversions, their functional roles in nitrogen metabolisms, and transcriptional responses to changes in DO concentration in the MAS system (**Fig. 7**).

Identification of AOM and amoA gene expression

No AOM MAG was recovered from the community, and metagenomic data confirmed the rare existence of the *Nitrosomonas amoA* gene in the MAS system. Operation under the microaerophilic condition successfully inhibited *amoA* expression; however, increasing DO concentration dramatically upregulated *amoA* expression, resulting in ammonia oxidation, congruent with the increase in nitrate concentration (**Fig. S1**). This finding agrees with AOB detection (but unnoticeable respiratory activities) by 16S rRNA amplicon sequencing, qPCR, and fluorescence *in situ* hybridization [5]. Hence, precise control of DO concentration was the key to retaining ammonia in the MAS system.

Genotypes and transcriptions of N_2O-reducing bacteria

The highest expression of clade II *nosZ* gene among nitrogen metabolism genes (**Fig. 4A**) highlighted the vital role in reducing N_2O under the microaerophilic condition (**Fig. 7**). This observation corroborates low or marginal N_2O emissions from the MAS system [5]. Crucial roles of clade II *nosZ* bacteria in N_2O reduction in WWTPs were previously reported [10, 58]. Repressing clade II *nosZ* gene expression at an elevated DO concentration likely explains the increased N_2O emissions observed in this study (**Fig. S1**) and our previous work [5].

The metatranscriptomics disclosed non-denitrifying bacteria belonging to Bacteroidota, particularly *Cloacibacterium*, as major N_2O sinks in the MAS system (**Figs. 5** and **7**). The *Cloacibacterium* highly expressed high-affinity terminal oxidase (*ccoNO*) and clade II *nosZ* (**Figs. 5** and **6**). *ccoNO* expression is instrumental in efficiently scavenging oxygen under

511 microaerophilic conditions, which conserves energy for bacterial growth and protects NosZ from
512 oxygen inhibition. The potential *nosZ* gene expression mechanism is congruent with a previous
513 work reporting oxygen uptake by oxygen-tolerant N_2O reducers [18]. Downregulation of both
514 *ccoNO* and clade II *nosZ* genes in these non-denitrifiers at a high DO concentration indicated
515 compromising N_2O reduction at an elevated DO concentration (**Fig. 7**). The phylogenetic tree of
516 *Cloacibacterium* species shows two distinctive branches; one contains the MAGs recovered in
517 this study (*Cloacibacterium* sp002422665 and *C. normanense*) and the other comprises
518 *Cloacibacterium* sp002337005 and *C. rupense* (**Fig. S4A**). The branch covering the two MAGs
519 in this study possesses *cnorB* and clade II *nosZ*, whereas the other branch (*Cloacibacterium*
520 sp002337005 and *C. rupense*) misses *norB* (**Fig. S4B**). All *Cloacibacterium* species possess
521 high-affinity terminal oxidase *cbb3*-type, while *C. rupense*, *C. caeni_A* (*a.k.a.* CB-01), *C.*
522 *caeni_B* (CB-03) [59], and *Cloacibacterium* sp002337005 additionally possess *cydBD*-type (**Fig.**
523 **S4B**), likely harboring the nature of oxygen tolerance.
524 *Cloacibacterium* is promising for N_2O mitigation in WWTPs. In a fed-batch experiment,
525 *Cloacibacterium* was enriched at a low N_2O concentration (20 ppmv in supplied gas) with a high
526 abundance, followed by *Flavobacterium* (Bacteroidota), while their abundances decreased at
527 higher N_2O concentrations [10]. The recently isolated *C. caeni_B* [59] showed a low growth rate
528 and affinity for N_2O but long-lasting persistence in soils despite the disadvantageous biokinetics
529 [15]. Non-denitrifying Bacteroidota were also predominant N_2O reducers in full-scale Danish
530 WWTPs [58, 60], in which N_2O concentration was below 1 mg/L. Additionally, uncultured *C.*
531 *normanense* was enriched in anaerobic pig manure digestate supplied with N_2O [61]. No nitrate
532 reduction was confirmed for the isolates of *C. normanense* NSR1 [62], *C. rupense* [63], and *C.*
533 *caeni* strain B6 [64]. Therefore, *Cloacibacterium* species are likely persistent non-denitrifying
534 N_2O sinks in the MAS system where limited amounts of N_2O and NO_3^- are available (**Fig. S1**). A
535 follow-up physiological investigation on the N_2O affinity of *Cloacibacterium* species isolated
536 from the system will clarify this claim.
537
538 ***DNRA bacteria and interaction with N_2O consumers***
539 The high *nrfA* gene expression found in this study likely facilitated the conversion of nitrite into
540 ammonia, resulting in high ammonia retention under microaerophilic conditions. We show that
541 *Chloroflexota* UBA8950 MAG (R1_bin54.o) exceptionally upregulated *nrfA* gene after

increasing DO concentration (**Fig. 5**), concomitant with the upregulation of *nirS*, *narG*, low-affinity terminal oxidase (*coxB*), and high-affinity terminal oxidase (*cydAB*) genes (**Figs. 5** and **6**). This expression pattern indicated that UBA8950 utilized different electron acceptors adaptable to alternating redox conditions. The genus UBA8950 currently comprises only two species (GTDB database, v207 Feb 2023) with five draft genomes (four for sp001872455 and one for sp002840685). All genomes were derived from groundwater metagenomes without the culture representative [40]. The UBA8950 MAG in this study was classified as a new species within this genus. The phylogenetic tree position of this MAG lies in the same branch with sp002840685 (**Fig. S5A**). Functional annotation showed that all UBA8950 genomes possess high-affinity (*cydBD*) and low-affinity (*cox*) oxidases. The UBA8950 MAG and sp002840685 genomes carry genes in nitrate reduction, nitrite reduction, and DNRA pathways, whereas genomes of sp001872455 do not (**Fig. S5B**). Isolation and physiological characterization of UBA8950 bacteria are required for the practical application of the MAS system.

Another notable finding in this study is the coexistence of N_2O reduction and DNRA pathways in the recovered MAGs. Approximately 26% of MAGs possessing clade II *nosZ* gene also harbor the *nrfA* gene, congruent with the previous report [8]. The high expression of the clade II *nosZ* gene and DNRA genes (*nrfA* and *octR*) by an unclassified UBA6192 species (R2_bin12.r) in Bacteridota (**Fig. 5**), taxonomically close to sp002421995 (**Fig. S6A**), suggests the contribution to N_2O reduction and DNRA in the MAS system. The *nrfA* expression remained unchanged at an elevated DO concentration, contributing to DNRA even under aerobic conditions. Despite carrying *nirK*, *cnorB*, and high-affinity *cbb3*-oxidases genes, the low gene expressions implied a minor contribution to N_2O production, underscoring that the UBA6192 MAG (R2_bin12.r) is an ideal candidate for improving N_2O mitigation and ammonia recovery, *i.e.*, reducing nitrate to ammonia. There are 17 draft genomes of 11 species in the GTDB database for the uncultured UBA6192 genus. All 11 species have the nitrite reduction pathway, and 7 species harbor DNRA and/or NO reduction, whereas only 2 species (sp018816765 and sp018336125) possess *nosZ* (**Fig. S6B**), showcasing the genotype uniqueness of UBA 6192 MAG (R2_bin12.r).

Another potential candidate to facilitate ammonia recovery is PGYU01 MAG (R2_bin45.o), displaying higher expressions of both *nrfA* and *octR* genes before increasing a DO concentration (**Fig. 5**). The downregulation of *nrfA* and *octR* genes and upregulation of *qnorB* and clade II *nosZ* genes at a high DO concentration suggests the switching function from DNRA to N_2O

reduction. Comparably high *nrfA* and *octR* gene expressions in UTCHB3 (Ignavibacteriaceae) bacteria, four MAGs recovered in this study with the genotypes allowing N_2O reduction and DNRA (**Fig. S7B**), indicate an active involvement in DNRA. Although these bacteria did not pronouncedly express *nosZ* compared to PGYU01 MAG, all UTCHB3 showed moderate *nrfA* expression (**Fig. 5**), potentially instrumental in reducing nitrite to ammonia. PGYU01 and UTCHB3 may support high ammonia recovery by reducing nitrite to ammonia when excessive aeration unwantedly enhances nitrification in the MAS system.

N-converting microorganisms in the presence of DO

The MAS system, supplied with high-strength nitrogenous wastewater, is rate-limited by oxygen supply. Increasing oxygen supply enhances organic carbon removal and, as a downside, initiates ammonia oxidation in conjunction with N_2O production by AOMs, as shown in **Fig. S1**. Exploring and harnessing bacteria exerting N_2O reduction and DNRA potentially paves the way towards high ammonia retention with low N_2O emissions. Our metatranscriptomic analysis allowed the classification of several phenotypical responses to an increase in DO concentration (**Fig. 7**).

The predominant bacterial members responsible for N_2O reduction and DNRA exhibited high gene expressions of high-affinity terminal oxidases (*ccoNO* or *cydAB*) and nitrogen oxide reductases. However, the preferential electron acceptor and the strategy for growth seem diverse. The concomitant decreases in high-affinity terminal oxidases *ccoNO* and clade II *nosZ* gene expressions of *Cloacibacterium* (**Figs. 5** and **6**) suggest that the effectiveness as an N_2O sink could be limited under high DO conditions. The downregulations of clade II *nosZ* and *octR* and the unchanged regulation of *nrfA* and *ccoNO* at a high DO concentration, observed in Bacteroidota UBA6192, indicate that N_2O reduction and DNRA are compromised after increasing DO concentrations. Much higher expressions of *nrfA* and *nirS* genes than *coxAB* and *cydAB* genes of Chloroflexota UBA8950 at a high DO concentration allude to utilizing nitrogen oxides as the primary electron acceptors and facilitating DNRA at a high DO concentration. Reportedly, DNRA, dependent on NrfA activity, proceeds under oxygen-limited conditions [65], although it may be less oxygen-sensitive than anticipated [66]. The highly expressed terminal oxidase gene (**Fig. 6**) may scavenge oxygen in the periplasm of Chloroflexota UBA8950. The underlying mechanism and the occurrence of DNRA warrant future investigations.

By combining online monitoring of the MAS system, metagenomic, and transcriptomic analyses, this study identified transcriptomically active bacteria responsible for high ammonia retention efficiency and low N_2O emissions in transitioning from microaerophilic to aerobic conditions. Our analysis revealed non-denitrifying N_2O-reducing bacteria affiliated with clade II *nosZ* *Cloacibacterium* in the phylum Bacterioidota as a promising N_2O sink in microaerophilic conditions. While *Cloacibacterium* decreased transcriptomic activities by transitioning from a microaerophilic to an aerobic condition, bacteria responsible for DNRA, *e.g.*, the genus UBA8950 (Chloroflexota), became active, likely switching from N_2O reduction to DNRA as a primary nitrogen transformation function of the microbial community at elevated oxygen levels. Switching such metabolic functions in the community of the MAS system caused by oxygen level transitions allowed high ammonia retention with fewer N_2O emissions even during dynamic oxygen fluctuations, which occasionally occurs in an engineered system for nitrogen management. Our findings may help achieve stable operation for ammonia recovery, a new paradigm that turns nitrogen removal into nitrogen recovery.

ACKNOWLEDGEMENTS

This paper was based on results obtained through the project of JPNP18016 commissioned by the New Energy and Industrial Technology Development Organization (NEDO). We thank Gabrielle White Wolf, PhD, from Edanz (https://jp.edanz.com/ac) for editing a draft of this manuscript.

COMPETING INTERESTS

There is no competing interest present.

DATA AVAILABILITY STATEMENT

The data of this study will be available upon request.

REFERENCES

1. Cruz H, Law YY, Guest JS *et al.* Mainstream ammonium recovery to advance sustainable urban wastewater management. *Environmental Science & Technology*. 2019;**53**:11066-79 https://doi.org/10.1021/acs.est.9b00603
2. Kartal B, Kuenen JG, van Loosdrecht MCM. Sewage treatment with anammox. *Science*. 2010;**328**:702-03 https://doi.org/doi:10.1126/science.1185941
3. Daelman MRJ, van Voorthuizen EM, van Dongen LGJM *et al.* Methane and nitrous oxide emissions from municipal wastewater treatment - results from a long-term study. *Water Science and Technology*. 2013;**67**:2350-55 https://doi.org/10.2166/wst.2013.109
4. Duan J, Van Phan H, Tsukamoto H *et al.* Microaerophilic activated sludge system for ammonia retention from high-strength nitrogenous wastewater: Biokinetics and mathematical modeling. *Biochemical Engineering Journal*. 2022:108790 https://doi.org/https://doi.org/10.1016/j.bej.2022.108790
5. Tsukamoto H, Phan HV, Suenaga T *et al.* Microaerophilic activated sludge system for ammonia retention toward recovery from high-strength nitrogenous wastewater: Performance and microbial communities. *Environmental Science & Technology*. 2023;**57**:13874-86 https://doi.org/10.1021/acs.est.3c03002
6. Wüst A, Schneider L, Pomowski A *et al.* Nature's way of handling a greenhouse gas: The copper-sulfur cluster of purple nitrous oxide reductase. *Biological Chemistry*. 2012;**393**:1067-77 https://doi.org/doi:10.1515/hsz-2012-0177
7. Jones CM, Graf DRH, Bru D *et al.* The unaccounted yet abundant nitrous oxide-reducing microbial community: A potential nitrous oxide sink. *The ISME Journal*. 2013;**7**:417-26 https://doi.org/10.1038/ismej.2012.125
8. Sanford RA, Wagner DD, Wu Q *et al.* Unexpected nondenitrifier nitrous oxide reductase gene diversity and abundance in soils. *Proceedings of the National Academy of Sciences*. 2012;**109**:19709-14 https://doi.org/doi:10.1073/pnas.1211238109
9. Graf DRH, Jones CM, Hallin S. Intergenomic comparisons highlight modularity of the denitrification pathway and underpin the importance of community structure for n2o emissions. *PLOS ONE*. 2014;**9**:e114118 https://doi.org/10.1371/journal.pone.0114118
10. Kim DD, Park D, Yoon H *et al.* Quantification of nosz genes and transcripts in activated sludge microbiomes with novel group-specific qpcr methods validated with metagenomic analyses. *Water Research*. 2020;**185**:116261 https://doi.org/https://doi.org/10.1016/j.watres.2020.116261
11. Suenaga T, Hori T, Riya S *et al.* Enrichment, isolation, and characterization of high-affinity n2o-reducing bacteria in a gas-permeable membrane reactor. *Environmental Science & Technology*. 2019;**53**:12101-12 https://doi.org/10.1021/acs.est.9b02237
12. Suenaga T, Riya S, Hosomi M *et al.* Biokinetic characterization and activities of n2o-reducing bacteria in response to various oxygen levels. *Frontiers in Microbiology*. 2018;**9** https://doi.org/10.3389/fmicb.2018.00697
13. Yoon S, Nissen S, Park D *et al.* Nitrous oxide reduction kinetics distinguish bacteria harboring clade i nosz from those harboring clade ii nosz. *Applied and Environmental Microbiology*. 2016;**82**:3793-800 https://doi.org/doi:10.1128/AEM.00409-16
14. Conthe M, Wittorf L, Kuenen JG *et al.* Life on n2o: Deciphering the ecophysiology of n2o respiring bacterial communities in a continuous culture. *The ISME Journal*. 2018;**12**:1142-53 https://doi.org/10.1038/s41396-018-0063-7

15. Hiis EG, Vick SHW, Molstad L *et al.* Unlocking bacterial potential to reduce farmland n2o emissions. *Nature*. 2024;**630**:421-28 https://doi.org/10.1038/s41586-024-07464-3
16. Bryson SJ, Hunt KA, Stahl DA *et al.* Metagenomic insights into competition between denitrification and dissimilatory nitrate reduction to ammonia within one-stage and two-stage partial-nitritation anammox bioreactor configurations. *Frontiers in Microbiology*. 2022;**13** https://doi.org/10.3389/fmicb.2022.825104
17. Kim DD, Han H, Yun T *et al.* Identification of nosz-expressing microorganisms consuming trace n2o in microaerobic chemostat consortia dominated by an uncultured burkholderiales. *The ISME Journal*. 2022;**16**:2087-98 https://doi.org/10.1038/s41396-022-01260-5
18. Wang Z, Vishwanathan N, Kowaliczko S *et al.* Clarifying microbial nitrous oxide reduction under aerobic conditions: Tolerant, intolerant, and sensitive. *Microbiology Spectrum.* 2023;**11**:e04709-22 https://doi.org/doi:10.1128/spectrum.04709-22
19. Zhou Y, Suenaga T, Qi C *et al.* Temperature and oxygen level determine n2o respiration activities of heterotrophic n2o-reducing bacteria: Biokinetic study. *Biotechnology and Bioengineering*. 2021;**118**:1330-41 https://doi.org/https://doi.org/10.1002/bit.27654
20. Atkinson SJ, Mowat CG, Reid GA *et al.* An octaheme c-type cytochrome from shewanella oneidensis can reduce nitrite and hydroxylamine. *FEBS Letters*. 2007;**581**:3805-08 https://doi.org/https://doi.org/10.1016/j.febslet.2007.07.005
21. Simon J, Klotz MG. Diversity and evolution of bioenergetic systems involved in microbial nitrogen compound transformations. *Biochimica et Biophysica Acta (BBA) - Bioenergetics*. 2013;**1827**:114-35 https://doi.org/https://doi.org/10.1016/j.bbabio.2012.07.005
22. Wang S, Liu C, Wang X *et al.* Dissimilatory nitrate reduction to ammonium (dnra) in traditional municipal wastewater treatment plants in china: Widespread but low contribution. *Water Research*. 2020;**179**:115877 https://doi.org/https://doi.org/10.1016/j.watres.2020.115877
23. Wan Y, Huang Z, Zhou L *et al.* Bioelectrochemical ammoniation coupled with microbial electrolysis for nitrogen recovery from nitrate in wastewater. *Environmental Science & Technology*. 2020;**54**:3002-11 https://doi.org/10.1021/acs.est.9b05290
24. Zhao Y, Li Q, Cui Q *et al.* Nitrogen recovery through fermentative dissimilatory nitrate reduction to ammonium (dnra): Carbon source comparison and metabolic pathway. *Chem Eng J*. 2022;**441**:135938 https://doi.org/https://doi.org/10.1016/j.cej.2022.135938
25. Kern M, Simon J. Three transcription regulators of the nss family mediate the adaptive response induced by nitrate, nitric oxide or nitrous oxide in wolinella succinogenes. *Environ Microbiol*. 2016;**18**:2899-912 https://doi.org/https://doi.org/10.1111/1462-2920.13060
26. Liu S, Dai J, Wei H *et al.* Dissimilatory nitrate reduction to ammonium (dnra) and denitrification pathways are leveraged by cyclic amp receptor protein (crp) paralogues based on electron donor/acceptor limitation in shewanella loihica pv-4. *Applied and Environmental Microbiology*. 2021;**87**:e01964-20 https://doi.org/doi:10.1128/AEM.01964-20
27. Yoon S, Cruz-García C, Sanford R *et al.* Denitrification versus respiratory ammonification: Environmental controls of two competing dissimilatory no3−/no2− reduction pathways in shewanella loihica strain pv-4. *The ISME Journal*. 2015;**9**:1093-104 https://doi.org/10.1038/ismej.2014.201

28. Butler JM Chapter 2 - DNA extraction methods. In: Butler JM (ed.). *Advanced topics in forensic DNA typing: Methodology*, San Diego: Academic Press. 29-47. Retreived from https://www.sciencedirect.com/science/article/pii/B9780123745132000026
29. Chen S, Zhou Y, Chen Y *et al*. Fastp: An ultra-fast all-in-one fastq preprocessor. *Bioinformatics*. 2018;**34**:i884-i90 https://doi.org/10.1093/bioinformatics/bty560
30. Li H, Durbin R. Fast and accurate short read alignment with burrows–wheeler transform. *Bioinformatics*. 2009;**25**:1754-60 https://doi.org/10.1093/bioinformatics/btp324
31. Li H, Handsaker B, Wysoker A *et al*. The sequence alignment/map format and samtools. *Bioinformatics*. 2009;**25**:2078-79 https://doi.org/10.1093/bioinformatics/btp352
32. Walker BJ, Abeel T, Shea T *et al.* Pilon: An integrated tool for comprehensive microbial variant detection and genome assembly improvement. *PLOS ONE*. 2014;**9**:e112963 https://doi.org/10.1371/journal.pone.0112963
33. Chen Y-H, Chiang P-W, Rogozin DY *et al.* Salvaging high-quality genomes of microbial species from a meromictic lake using a hybrid sequencing approach. *Communications Biology*. 2021;**4**:996 https://doi.org/10.1038/s42003-021-02510-6
34. Chakraborty M, Baldwin-Brown JG, Long AD *et al*. Contiguous and accurate de novo assembly of metazoan genomes with modest long read coverage. *Nucleic Acids Research*. 2016;**44**:e147-e47 https://doi.org/10.1093/nar/gkw654
35. Uritskiy GV, DiRuggiero J, Taylor J. Metawrap—a flexible pipeline for genome-resolved metagenomic data analysis. *Microbiome*. 2018;**6**:158 https://doi.org/10.1186/s40168-018-0541-1
36. Alneberg J, Bjarnason BS, de Bruijn I *et al.* Binning metagenomic contigs by coverage and composition. *Nature Methods*. 2014;**11**:1144-46 https://doi.org/10.1038/nmeth.3103
37. Wu Y-W, Simmons BA, Singer SW. Maxbin 2.0: An automated binning algorithm to recover genomes from multiple metagenomic datasets. *Bioinformatics*. 2015;**32**:605-07 https://doi.org/10.1093/bioinformatics/btv638
38. Kang DD, Li F, Kirton E *et al.* Metabat 2: An adaptive binning algorithm for robust and efficient genome reconstruction from metagenome assemblies. *PeerJ*. 2019;**7**:e7359 https://doi.org/10.7717/peerj.7359
39. Nissen JN, Johansen J, Allesøe RL *et al.* Improved metagenome binning and assembly using deep variational autoencoders. *Nature Biotechnology*. 2021;**39**:555-60 https://doi.org/10.1038/s41587-020-00777-4
40. Parks DH, Chuvochina M, Waite DW *et al.* A standardized bacterial taxonomy based on genome phylogeny substantially revises the tree of life. *Nature Biotechnology*. 2018;**36**:996-1004 https://doi.org/10.1038/nbt.4229
41. Olm MR, Brown CT, Brooks B *et al.* Drep: A tool for fast and accurate genomic comparisons that enables improved genome recovery from metagenomes through de-replication. *The ISME Journal*. 2017;**11**:2864-68 https://doi.org/10.1038/ismej.2017.126
42. Chaumeil P-A, Mussig AJ, Hugenholtz P *et al.* Gtdb-tk: A toolkit to classify genomes with the genome taxonomy database. *Bioinformatics*. 2019;**36**:1925-27 https://doi.org/10.1093/bioinformatics/btz848
43. Parks DH, Chuvochina M, Chaumeil P-A *et al.* A complete domain-to-species taxonomy for bacteria and archaea. *Nature Biotechnology*. 2020;**38**:1079-86 https://doi.org/10.1038/s41587-020-0501-8

44. Pérez-Rubio P, Lottaz C, Engelmann JC. Fastqpuri: High-performance preprocessing of rna-seq data. *BMC Bioinformatics*. 2019;**20**:226 https://doi.org/10.1186/s12859-019-2799-0
45. Kopylova E, Noé L, Touzet H. Sortmerna: Fast and accurate filtering of ribosomal rnas in metatranscriptomic data. *Bioinformatics*. 2012;**28**:3211-17 https://doi.org/10.1093/bioinformatics/bts611
46. Seemann T. Prokka: Rapid prokaryotic genome annotation. *Bioinformatics*. 2014;**30**:2068-69 https://doi.org/10.1093/bioinformatics/btu153
47. Zhou Z, Tran PQ, Breister AM *et al.* Metabolic: High-throughput profiling of microbial genomes for functional traits, metabolism, biogeochemistry, and community-scale functional networks. *Microbiome*. 2022;**10**:33 https://doi.org/10.1186/s40168-021-01213-8
48. Morris RL, Schmidt TM. Shallow breathing: Bacterial life at low o2. *Nature Reviews Microbiology*. 2013;**11**:205-12 https://doi.org/10.1038/nrmicro2970
49. Fish JA, Chai B, Wang Q *et al.* Fungene: The functional gene pipeline and repository. *Frontiers in Microbiology*. 2013;**4**
50. Milanese A, Mende DR, Paoli L *et al.* Microbial abundance, activity and population genomic profiling with motus2. *Nature Communications*. 2019;**10**:1014 https://doi.org/10.1038/s41467-019-08844-4
51. Salazar G, Paoli L, Alberti A *et al.* Gene expression changes and community turnover differentially shape the global ocean metatranscriptome. *Cell*. 2019;**179**:1068-83.e21 https://doi.org/https://doi.org/10.1016/j.cell.2019.10.014
52. Wagner GP, Kin K, Lynch VJ. Measurement of mrna abundance using rna-seq data: Rpkm measure is inconsistent among samples. *Theory in Biosciences*. 2012;**131**:281-85 https://doi.org/10.1007/s12064-012-0162-3
53. Langmead B, Salzberg SL. Fast gapped-read alignment with bowtie 2. *Nature Methods*. 2012;**9**:357-59 https://doi.org/10.1038/nmeth.1923
54. Love MI, Huber W, Anders S. Moderated estimation of fold change and dispersion for rna-seq data with deseq2. *Genome Biology*. 2014;**15**:550 https://doi.org/10.1186/s13059-014-0550-8
55. Edgar RC. Muscle: A multiple sequence alignment method with reduced time and space complexity. *BMC Bioinformatics*. 2004;**5**:113 https://doi.org/10.1186/1471-2105-5-113
56. Minh BQ, Schmidt HA, Chernomor O *et al.* Iq-tree 2: New models and efficient methods for phylogenetic inference in the genomic era. *Molecular Biology and Evolution*. 2020;**37**:1530-34 https://doi.org/10.1093/molbev/msaa015
57. Podosokorskaya OA, Kadnikov VV, Gavrilov SN *et al.* Characterization of melioribacter roseus gen. Nov., sp. Nov., a novel facultatively anaerobic thermophilic cellulolytic bacterium from the class ignavibacteria, and a proposal of a novel bacterial phylum ignavibacteriae. *Environ Microbiol*. 2013;**15**:1759-71 https://doi.org/https://doi.org/10.1111/1462-2920.12067
58. Valk LC, Peces M, Singleton CM *et al.* Exploring the microbial influence on seasonal nitrous oxide concentration in a full-scale wastewater treatment plant using metagenome assembled genomes. *Water Research*. 2022;**219**:118563 https://doi.org/https://doi.org/10.1016/j.watres.2022.118563

59. Jonassen KR, Ormåsen I, Duffner C *et al.* A dual enrichment strategy provides soil- and digestate-competent nitrous oxide-respiring bacteria for mitigating climate forcing in agriculture. *mBio*. 2022;**13**:e00788-22 https://doi.org/doi:10.1128/mbio.00788-22
60. Singleton CM, Petriglieri F, Kristensen JM *et al.* Connecting structure to function with the recovery of over 1000 high-quality metagenome-assembled genomes from activated sludge using long-read sequencing. *Nature Communications*. 2021;**12**:2009 https://doi.org/10.1038/s41467-021-22203-2
61. Wang X, Xiang B, Zhang M *et al.* Sixteen genome sequences of denitrifying bacteria assembled from enriched cultures of anaerobic pig manure digestate. *Microbiology Resource Announcements*. 2021;**10**:e00782-21 https://doi.org/doi:10.1128/MRA.00782-21
62. Allen TD, Lawson PA, Collins MD *et al.* Cloacibacterium normanense gen. Nov., sp. Nov., a novel bacterium in the family flavobacteriaceae isolated from municipal wastewater. *International Journal of Systematic and Evolutionary Microbiology*. 2006;**56**:1311-16 https://doi.org/https://doi.org/10.1099/ijs.0.64218-0
63. Cao S-J, Deng C-P, Li B-Z *et al.* Cloacibacterium rupense sp. Nov., isolated from freshwater lake sediment. *International Journal of Systematic and Evolutionary Microbiology*. 2010;**60**:2023-26 https://doi.org/https://doi.org/10.1099/ijs.0.017681-0
64. Chun BH, Lee Y, Jin HM *et al.* Cloacibacterium caeni sp. Nov., isolated from activated sludge. *International Journal of Systematic and Evolutionary Microbiology*. 2017;**67**:1688-92 https://doi.org/https://doi.org/10.1099/ijsem.0.001841
65. Saghaï A, Hallin S. Diversity and ecology of nrfa-dependent ammonifying microorganisms. *Trends in Microbiology*. 2024;**32**:602-13 https://doi.org/10.1016/j.tim.2024.02.007
66. Pett-Ridge J, Silver WL, Firestone MK. Redox fluctuations frame microbial community impacts on n-cycling rates in a humid tropical forest soil. *Biogeochemistry*. 2006;**81**:95-110 https://doi.org/10.1007/s10533-006-9032-8

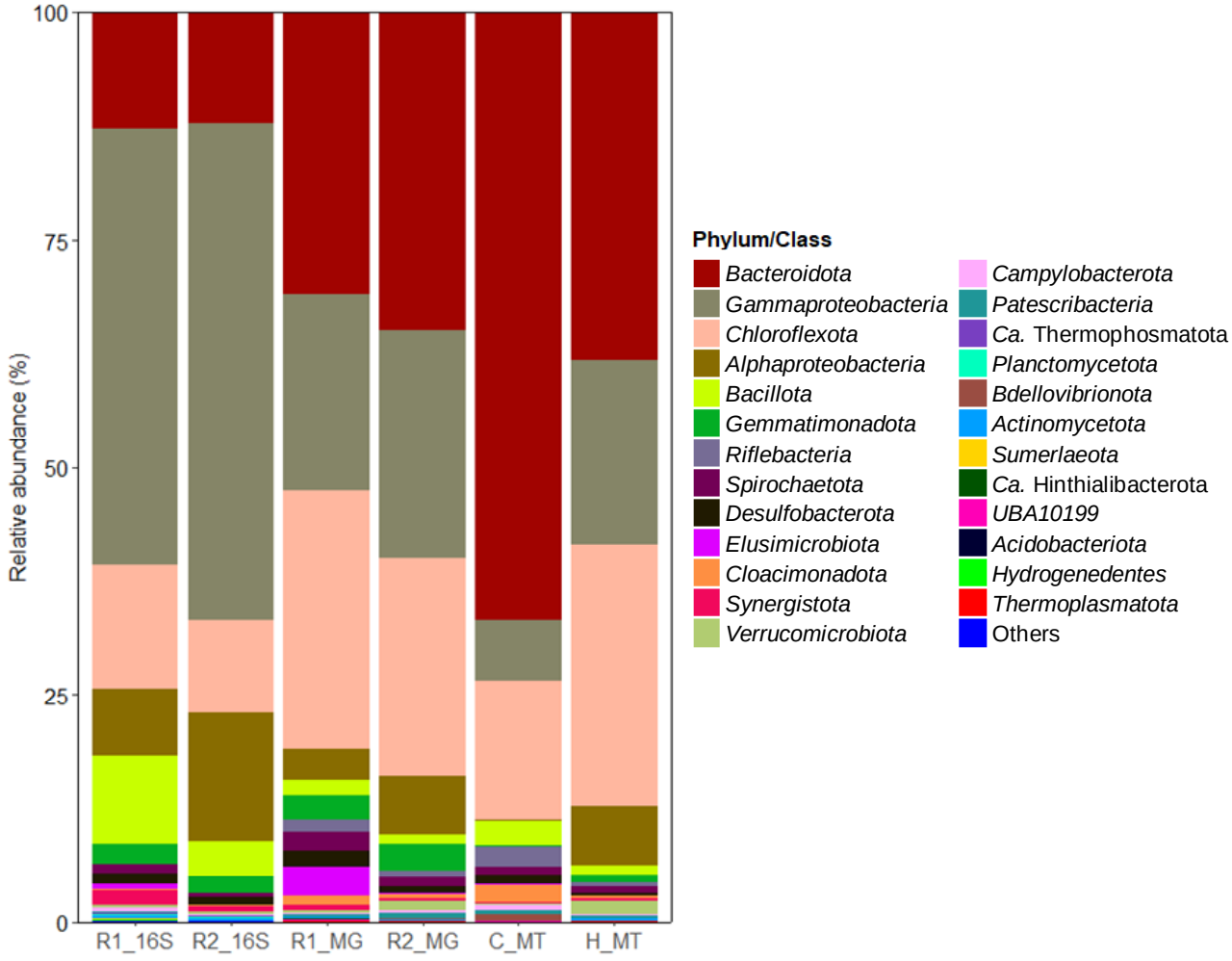

Figure 1: Relative abundance and mRNA expression profiles of microbial community at phylum (class level for Proteobacteria) level in microaerophilic activated sludge systems based on amplicon sequencing of the V4 region in the 16S rRNA gene (R1_16S and R2_16S), metagenome-assembled genomes (MAGs) (R1_MG and R2_MG), and metatranscriptomic reads of reactor 2 (R2) under microaerophilic (C_MT) and high DO (H_MT) conditions mapped to MAGs. Bacterial phyla with abundance < 0.03% were grouped into Others.

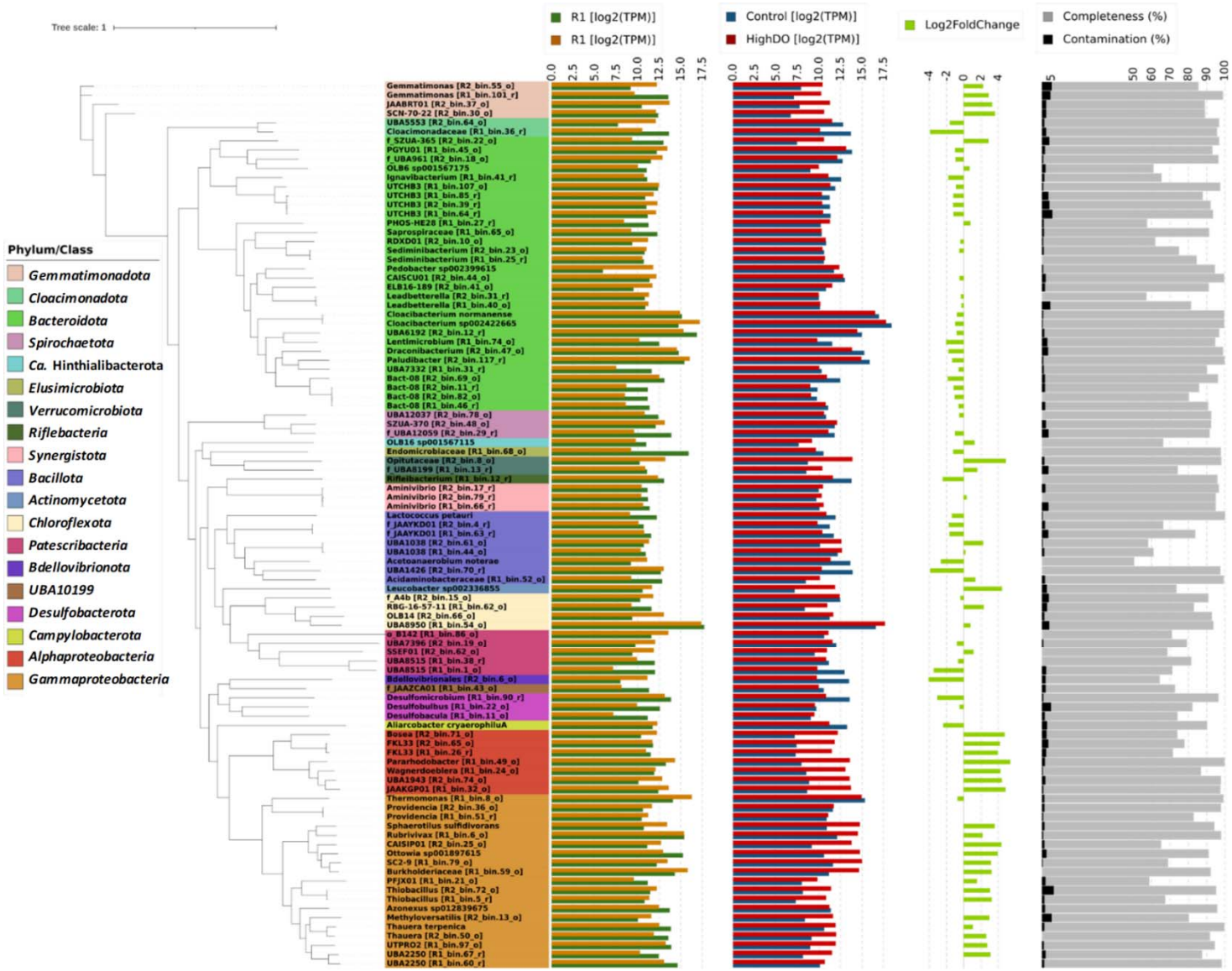

Figure 2: The phylogenomic tree of 97 bacterial metagenome-assembled genomes (MAGs) recovered from this study. The phyla in the tree are colored, whereas the phylum Proteobacteria is further broken down into a class level. The tip labels are the lowest taxonomic classification of MAGs by GTDB-tk (v1.7.0) with GTDB R202. The MAG IDs are included in the square brackets, except for MAGs, which are assigned with species names. The innermost bar plots show the relative abundance (log_2TPM) of MAGs recovered from metagenomics data of R1 (green) and R2 (orange). The second innermost bar plots represent the average mRNA expression (log_2TPM) of MAGs in metatranscriptomics data of triplicate biomass samples from R2 under microaerophilic (control, dark blue) and high dissolved oxygen (red) conditions. The next column in light green is the normalized mRNA expression [log_2 foldchange (High DO/Control)] over the control value as the denominator, calculated by DEseq2. Only statistically different values (adj *p-value* < 0.05) are shown. The outermost bar plots show the contamination (black, maximum value = 6.26%) and completeness (light grey) of MAGs by CheckM. The tree was constructed by IQ-TREE2 (v2.2.0) using multiple sequence alignment of 120 bacterial marker genes generated by "classify_wf" of GTDB-tk.

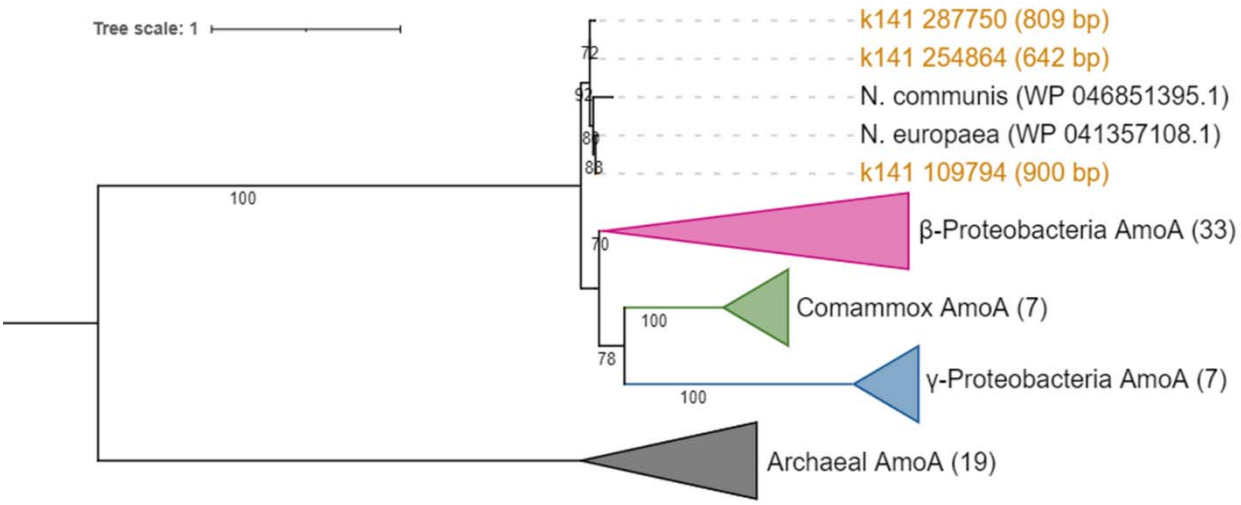

Figure 3: Phylogenetic tree of ammonia monooxygenase subunit A (AmoA) proteins. Amino acid sequences obtained in this study are shown in orange. The lengths of nucleotide sequences (bp) are included in parentheses. The reference AmoA sequences for AOB, Comammox, and AOA were downloaded (seed sequences) from FunGene (http://fungene.cme.msu.edu/, accessed date: 23 March 2022). The number of reference sequences in the collapse clades is indicated in each parenthesis. The bootstrap numbers (1000 replicates) are shown along the branches. The scale bar indicates estimated substitutions of amino acids. The tree was rooted at the midpoint.

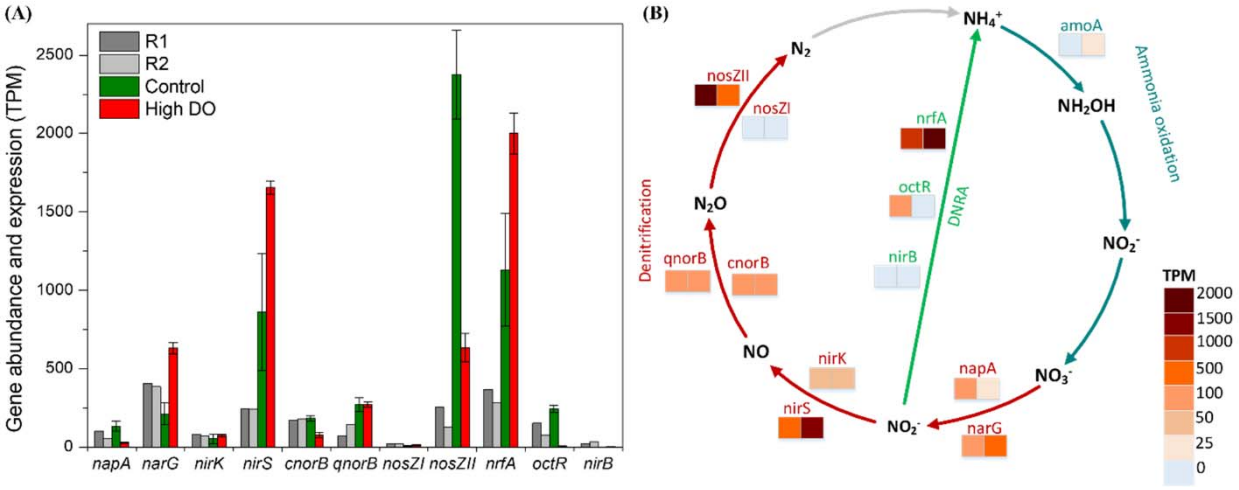

Figure 4: (**A**) Relative abundance (metagenomics R1 and R2) and expression (metatranscriptomics control and high DO) of nitrate respiration genes. Values represent transcripts per million (TPM). Error bars represent the standard deviation of triplicate metatranscriptomic samples. **(B)** A diagram of nitrogen metabolisms in the MAS system: nitrification (dark green), denitrification (dark red), and DNRA (light green). Heatmap color bars indicate the expression level of genes (transcriptomics) with control in the left squares and high DO in the right squares.

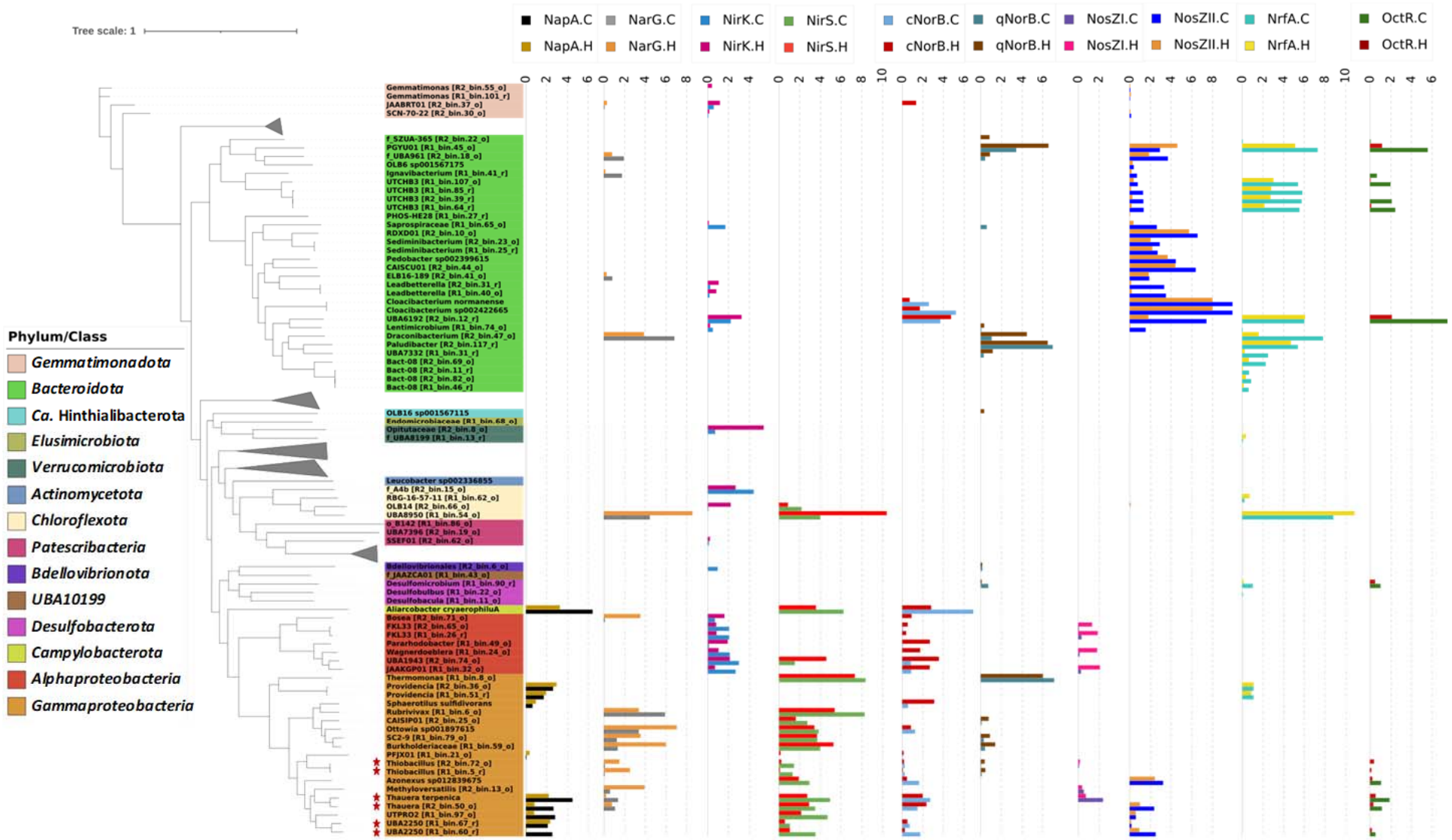

Figure 5: The expression of nitrogen cycle-associated genes of metagenome-assembled genomes (MAGs) obtained from a MAS system. The gene expression was expressed as $\log_2$(TPM+1). The "*" indicates MAGs possessing all denitrifying genes (canonical complete denitrifying bacteria).

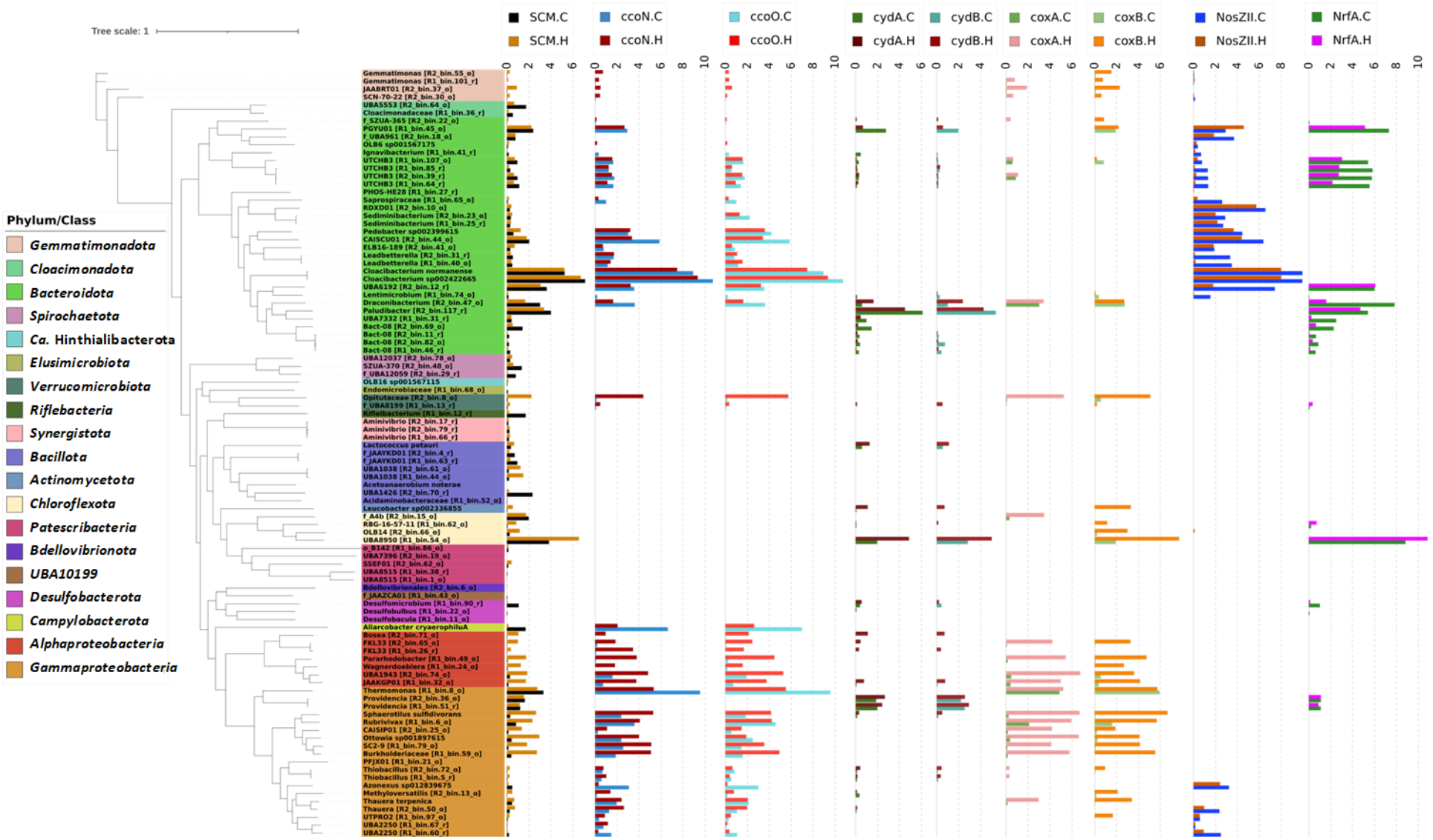

Figure 6: Transcript abundances of high-affinity terminal oxidases (*ccoNO* and *cydAB*) and low-affinity terminal oxidases (*coxAB*) in comparison with transcript abundances of clade II *nosZ* (NosZII), *nrfA*, and single copy markers (SCM). "C" and "H" represent control and high DO conditions, respectively. The gene expression was expressed as $\log_2$(TPM+1). The TPM value of SCM is the median TPM of the 10 selected SCMs.

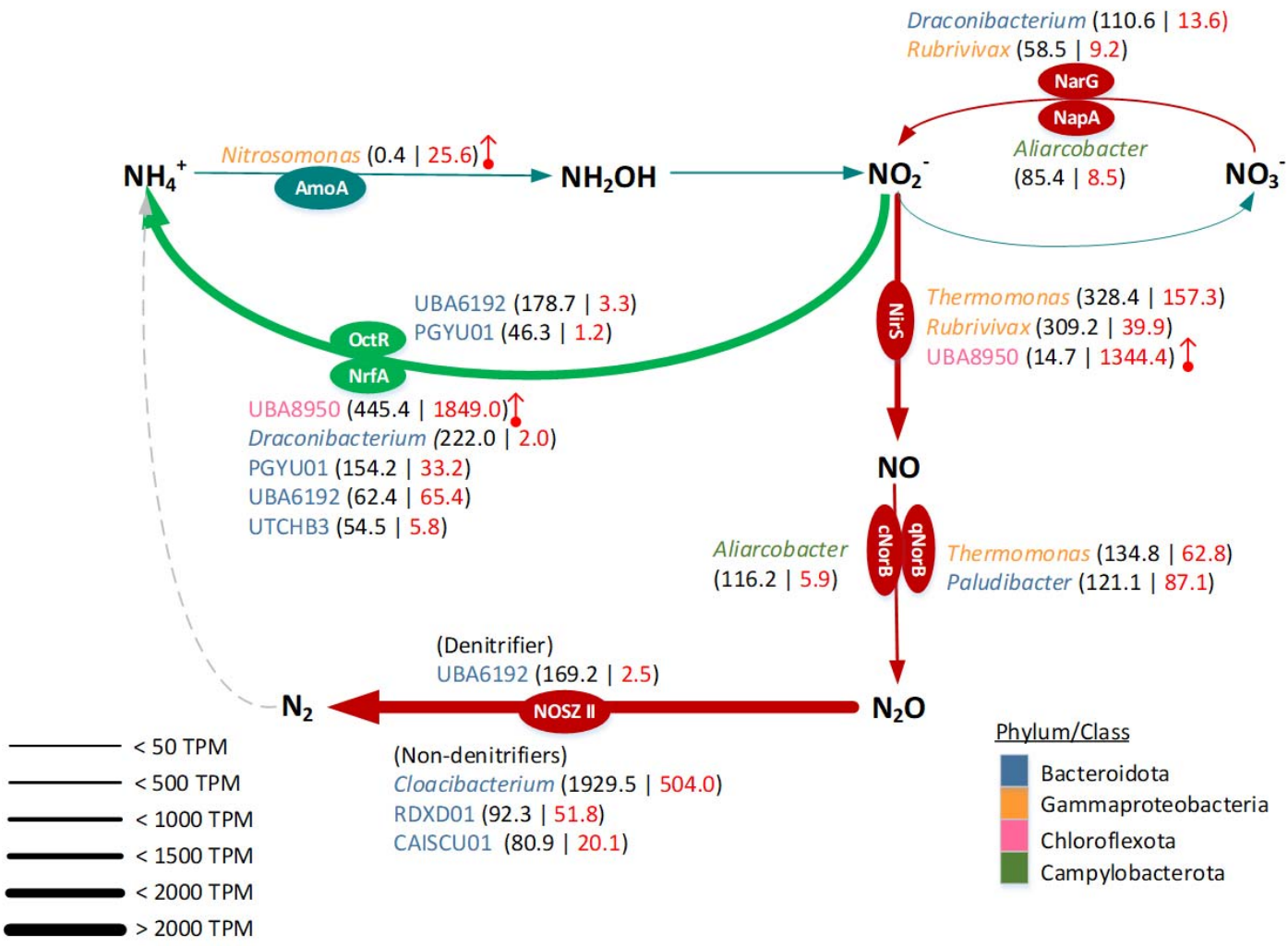

Figure 7: Diagram illustrating the contribution of pivotal microbial members to nitrogen transformations in the MAS system. Three key pathways, nitrification (dark green), denitrification (dark red), and DNRA (light green), with the key enzymes detected in metatranscriptomic data, are shown. The thickness of each continuous arrow indicates the transcription level of an assigned metabolic pathway of nitrogen transformation in the community. The microbial members responsible for each pathway are appended and colored according to phylum/class. The numbers in parentheses show the transcripts (> 45 TPM) of the key enzymes from each microbial member under control (left in black) and high DO (right in red) conditions. The remarkable gene upregulation under a high DO condition is highlighted by a vertical red arrow.

Table 1: The relative abundance and expression of the *amoA* gene, expressed as TPM (normalized to the gene length and total reads mapped to the sample).

Contig	Metagenomics		Metatranscriptomics					
	R1	R2	Control 1	Control 2	Control 3	High DO 1	High DO 2	High DO 3
k141_254864 (642 bp)	0.03	0.00	0.04	0.07	0.00	0.11	0.15	0.22
k141_109794 (900 bp)	0.09	0.19	0.02	0.84	0.22	17.53	20.61	19.46
k141_287750 (809 bp)	0.04	0.15	0.00	0.10	0.05	7.49	8.32	2.97
Sum	0.16	0.34	0.05	1.01	0.27	25.13	29.09	22.65